How to cite: Angew. Chem. Int. Ed. 2024, e202404878
doi.org/10.1002/anie.202404878

Molecular Switches Hot Paper

Orthogonal Photoswitching in a Porous Organic Framework

Jinyu Sheng, Jacopo Perego, Silvia Bracco, Piotr Cieciórski, Wojciech Danowski, Angiolina Comotti,* and Ben L. Feringa**

Abstract: The development of photoresponsive systems with non-invasive orthogonal control by distinct wavelengths of light is still in its infancy. In particular, the design of photochemically triggered-orthogonal systems integrated into solid materials that enable multiple dynamic control over their properties remains a long-standing challenge. Here, we report the orthogonal and reversible control of two types of photoswitches in an integrated solid porous framework, that is, visible-light responsive *o*-fluoroazobenzene and nitro-spiropyran motifs. The properties of the constructed material can be selectively controlled by different wavelengths of light thus generating four distinct states providing a basis for dynamic multifunctional materials. Solid-state NMR spectroscopy demonstrated the selective transformation of the azobenzene switch in the bulk, which in turn modulates N_2 and CO_2 adsorption.

The development of molecular switches enabled an unprecedented degree of control over molecular geometry in distinct environments ranging from solutions to solids.[1,2] However, most of these artificial systems show rather simple responsive behaviour, while the quest to mimic or rival the complexity of adaptive biological counterparts requires the development of more sophisticated architectures which show several distinct addressable states. In this regard, the combination of multiple responsive components driven by orthogonal stimuli allows to address each species with high selectivity and thus achieve far more advanced tasks than in a bistable system.[3–6] Fabrication of such dynamic architectures driven by the combination of multiple orthogonal physical or chemical stimuli has been explored in adaptive materials including functionalized surfaces, polymers, gels, or polymeric networks.[7–12] However, using light as an exclusive external stimulus is highly beneficial as it allows for remote control of the properties in a non-invasive manner with high spatiotemporal precision (Figure 1a).[3]

Wavelength-orthogonality can be readily engineered for light-irreversible reactions encompassing photo-uncaging[13] and photo-ligations reactions,[14] commonly employed in construction and control over properties of polymeric networks[15–17] or functionalisation of nanoparticles.[18] Despite these developments, achieving high selectivity and orthogonality of photoreactions in an architecture comprising multiple photoswitchable elements remains

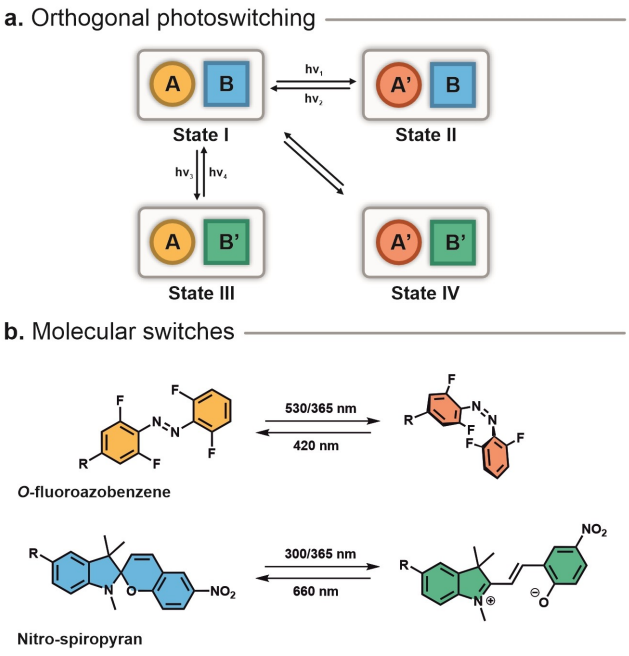

Figure 1. **a**. Concept of wavelength-selective orthogonal photoswitching. **b**. *O*-Fluoroazobenzene and nitro-spiropyran structures were applied in this work.

[*] Dr. J. Sheng, Dr. W. Danowski, Prof. B. L. Feringa
Stratingh Institute for Chemistry, University of Groningen, Nijenborgh 4, 9747 AG Groningen, Netherlands
E-mail: danowski@unistra.fr
b.l.feringa@rug.nl

Dr. J. Perego, Prof. S. Bracco, Prof. A. Comotti
Department of Materials Science, University of Milano Bicocca, Milan, Italy, Via R. Cozzi 55, Milan 20125, Italy
E-mail: angiolina.comotti@unimib.it

P. Cieciórski, Dr. W. Danowski
Faculty of Chemistry, University of Warsaw, Pasteura 1, 02-093 Warsaw, Poland

Dr. W. Danowski
Université de Strasbourg, CNRS, ISIS, 8 allée Gaspard Monge, 67000 Strasbourg, France

Dr. J. Sheng
Present address: Institute of Science and Technology Austria, Am Campus 1, 3400 Klosterneuburg, Austria

challenging.[4] Typical strategies rely on sufficient spectral separation between the chromophores. Therefore, the choice of available photoswitches is drastically limited as most of the commonly employed scaffolds feature overlapping absorption bands in the ultraviolet-visible region. Furthermore, the undesired intermolecular energy transfer between the chromophores can severely hamper the selectivity of these systems.[19] Pioneering studies provided several hybrids based predominantly on fulgides or dithienylethenes capable of switching between four independent states under irradiation with distinct light wavelengths.[20–23] More recently, azobenzene and/or visible-light-driven donor-acceptor Stenhouse adducts (DASA) photoswitches were proven suitable candidates for the fabrication of orthogonal systems in solution.[24–27] Despite a few examples of limited wavelength-selectivity for the pairs of photoswitches anchored to surfaces[28] or encapsulated in molecular cages,[29] most of these dyads were demonstrated to function solely in a diluted solution. However, the integration of these multistate systems into a material framework could unlock access to additional states with unique properties, thereby significantly enhancing their adaptability and as such constitutes a great challenge.

In recent decades, porous solids[30–32] have attracted major attention owing to their prominent properties in applications such as gas storage, separation, controlled delivery systems and environmental purification.[33–35] The presence of void pores in these structures generates the free volume necessary to facilitate molecular motion and accommodate geometrical changes associated with the photoisomerization of the incorporated photoresponsive units.[36] Concurrently, the isomerization of the photoswitches can affect the pore environment, leading to drastic changes in the properties of the material. However, incorporation of these moieties in the confined space may have a substantial impact on their photochemistry.[37–41] Additionally, the limited light-penetration depth in optically dense solids imposes intrinsic constrains to the operational efficiency of these materials. Despite these limitations, the fabrication of thin films or incorporation of the photoswitches with large spectral separation between both isomeric forms allows to circumvent this issue and fabricate materials that undergo quantitative isomerization in the bulk samples.[42–45]

Therefore, these porous structures constitute an ideal platform for the construction of light-responsive materials capable of harnessing limited changes in molecular geometry and transforming them into practical output.[36,46] Successful incorporation of single molecular photoswitches such as spiropyrans,[47–53] azobenzenes,[54–57] diarylethenes[58–60] and overcrowded alkenes[44,61–65] into these structures generated a plethora of porous materials with switchable properties including electronic or ionic conductivity, gas uptake or ion capture. Despite these advances, all these materials operate by switching between only two states of the incorporated responsive molecules while, orthogonal photoswitching in solid state to alter multiple states of a single material remains rarely explored.[66]

Here, we report the incorporation of *o*-fluoroazobenzene[67] and 5-nitro-spiropyran[68] (Figure 1b) in a porous aromatic framework (PAF) capable of working independently from each other, that is in a wavelength-orthogonal manner. The porous aromatic framework was fabricated using a Suzuki cross-coupling reaction between responsive monomers and tetraphenylmethane-based porogenic units. Both chromophores were designed based on a tritopic (see **S1**, **S2** on Scheme 1) tetraphenylmethane-derived unit ensuring the intrinsic three-dimensional (3D)

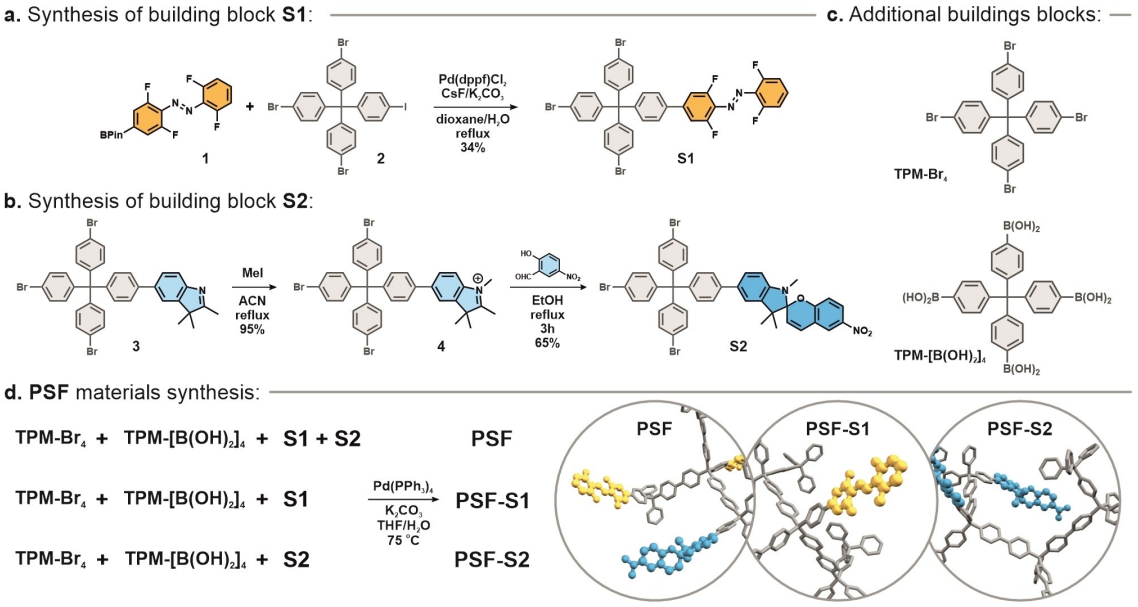

Scheme 1. Synthesis of **a**. *o*-fluoroazobenzene (**S1**) and **b**. nitro-spiropyran (**S2**) photoswitches. **c**. Structures of additional porogens **TPM-Br$_4$** and **TPM-[B(OH)$_2$]$_4$** **d**. Synthesis of **PSF-S1**, **PSF-S2** and **PSF** materials by a Suzuki cross-coupling polymerization reaction.

structure (Scheme 1a, b) which in turn should maintain the high porosity (pore capacity) of the framework.

The visible-light-responsive tribrominated azobenzene building block **S1** was synthesized via Suzuki-coupling reaction between a boronic ester-appended azobenzene **1** and mixed-halide tetraphenylmethane **2** (Scheme 1a). For the spiropyran synthesis, first, the tribrominated indole **3** was synthesized following a similar strategy to **1**. Next, the use of methylated indole **4** and the condensation with 5-nitrosalicylic aldehyde furnished the building block **S2** (Scheme 1b). Finally, the porous switchable framework (**PSF**) (Scheme 1d) was synthesized by a cross-coupling of tribrominated functional monomers and tetrabrominated porogenic unit (**TPM-Br$_4$**) with a porogenic tetratopic boronic acid derived from tetraphenylmethane (**TPM-[B-(OH)$_2$)$_4$]**) (Scheme 1c). Additional **TPM-Br$_4$** was used to ensure sufficient dilution and separation of the photoswitches in the framework to avoid undesired energy transfer and to maximize the light penetration depth. Two reference materials, i.e., **PSF-S1** and **PSF-S2**, were synthesized for comparison to the **PSF** material (Scheme 1d). After the synthesis, the framework materials were extensively washed with solvents (THF, H_2O, MeOH, CH_2Cl_2 and THF) to remove the unreacted monomers and by-products and activated under dynamic vacuum at 80 °C overnight (see Supporting Information synthesis section for further details).

The successful framework construction was confirmed by diffuse reflectance infrared Fourier transform spectroscopy (DRIFTS). The spectrum revealed the presence of bands centered at 1030 and 1050 cm^{-1} characteristic of –C–N= stretching, indicating the successful incorporation of the azobenzene functionality (Figure 2a). In addition, an intense band was observed at 1340 cm^{-1} characteristic of the –NO_2 group stretching, confirming incorporation of spiropyran unit in the framework (Figure 2a, see Figure S1 for comparison of DRIFT spectra **PSF-S1** and **PSF-S2**). The structure of the **PSF** appended with two photoswitches was further confirmed by solid-state ^{13}C NMR and ^{19}F NMR. The resonances in ^{1}H–^{13}C CP MAS NMR spectrum at $\delta =$ 29.5, 26.5 and 19.2 ppm, arising from the aliphatic carbons of spiropyran (Figure 2b), and the resonances at $\delta = 156.0$ and 131.5 ppm in ^{19}F–^{13}C CP MAS NMR experiment associated to the *o*-fluoroazobenzene units (Figure 2b, inset), as well as the single resonance at $\delta = -122.9$ ppm in ^{19}F MAS NMR (Figure S2), demonstrated the successful insertion of both photoswitches in the aromatic framework (see Table S1 for assignment of resonances). The corresponding groups of resonances were observed in ^{1}H–^{13}C CP MAS NMR of reference **PSF-S1** and **PSF-S2** frameworks further confirming the assignment (Figure S3, S4). The N_2 sorption isotherm collected at 77 K displays a type I (Langmuir) profile, typical of microporous materials (Figure 2c). Indeed, the pore size distribution calculated according to the NLDFT theory shows a relatively narrow pore size distribution centred at 7.5 nm. The Brunauer–Emmett–Teller (BET) and Langmuir surface areas of **PSF** are 612 m^2 g^{-1} and 677 m^2 g^{-1}, respectively, which was well-reproduced between two distinct batches (Figure S29, Table S3). The thermal stability of **PSF**

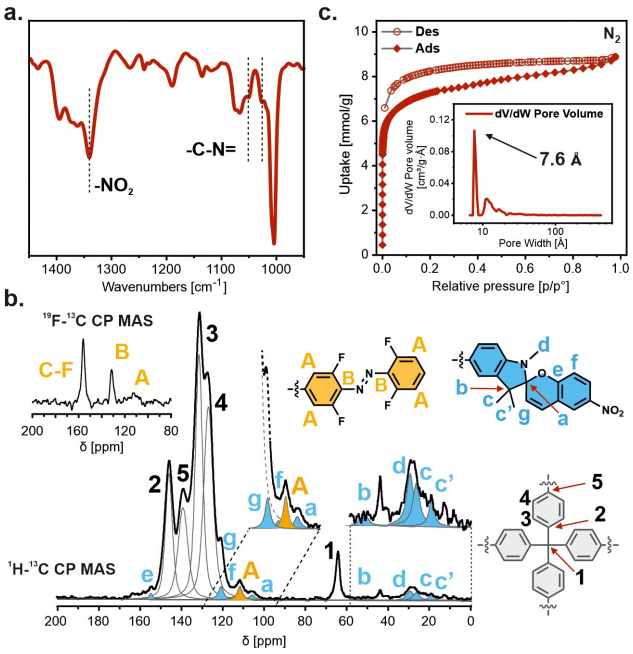

Figure 2. **a**. DRIFT spectrum of PSF. **b**. ^{13}C–^{1}H CP MAS spectrum of PSF with a contact time of 2 ms and ^{13}C–^{19}F CP MAS spectrum of PSF material collected with a contact time of 5 ms (inset, left above). The experiments were performed at 298 K at a spinning speed of 12.5 kHz. **c**. N_2 sorption isotherm collected at 77 K (filled diamonds and empty circles correspond to the adsorption and desorption branches, respectively). The inset shows the pore size distribution between 5 and 500 Å (logarithmic scale).

was verified with thermogravimetric analysis (TGA) under air which showed no mass loss up to 300 °C (Figure S5). Powder X-ray diffraction (PXRD) measurements (Figure S6) revealed no long-range order in the material and scanning electron microscopy (SEM) images showed that the materials consist of uniform spheres ca. <1 µm in diameter (Figure S7). Consistently, **PSF-S1** and **PSF-S2** showed similar morphology in SEM and N_2 sorption isotherms (Figure S7 and S9–10, Table S2).

Ultraviolet–visible (UV/Vis) absorption spectroscopy of photoswitches **S1** and **S2** ($1\cdot10^{-5}$ M each) in THF showed high wavelength orthogonality of both photoswitches. Irradiation of this mixture at 530 nm leads to a hypsochromic shift of the absorption band centred at 450 nm accompanied by a small decrease in absorption at shorter wavelengths (ca. 320 nm), consistent with a selective $E \rightarrow Z$ isomerization (Figure 3a) of the azobenzene photoswitch **S1**, which was further confirmed by downfield shift of ^{19}F resonances of **S2** (Figure S11). The long half-life of the *Z*-isomer of azobenzene **S1** (estimated $t_{1/2} > 200$ days at room temperature; Figure S12) renders the ***Z*-S1** thermally stable within the timeframe of the experiment. Subsequent irradiation of the mixture at 420 nm reverted these changes, proving selective $Z \rightarrow E$ back photoisomerization (Figure 3b). Throughout both processes, isosbestic points were maintained at 450 nm indicating clean unimolecular photoisomerization proceeding without affecting spiropyran photoswitch **S2** (Figure 3a and 3b insets). Spiropyran **S2** in this multicomponent system

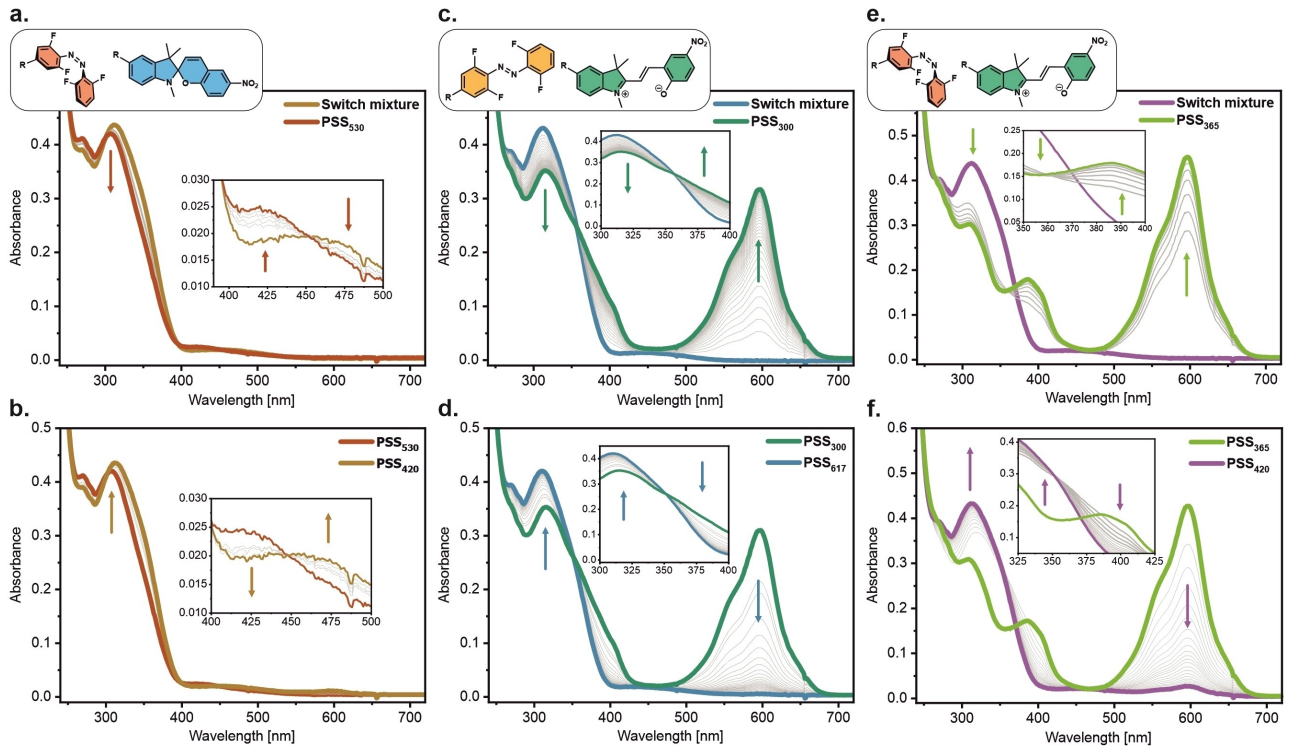

Figure 3. Orthogonal photoswitching in an intermolecular solution system. Reversible photoswitching of switch **S1** by **a**. 530 nm and **b**. 420 nm light manipulation; Ring-opening and closure isomerization of switch **S2** by **c**. 300 nm and **d**. 617 nm light irradiation; Simultaneous activation of switch **S1** and **S2** by **e**. 365 nm light irradiation and back isomerization by **f**. 420 nm light irradiation. For consistency, spectra in panels (e) and (f) were recorded with the same time interval (30 s) which precludes observation of intermediate spectra associated with photoisomerization of azobenzene (Figure S17 and S21).

could be selectively opened to the merocyanine form by irradiation at 300 nm (Figure 3c), upon which a new band cantered at ca. 600 nm emerged, characteristic of the open merocyanine form. The half-life of the merocyanine of **S2** in THF was relatively short (estimated $t_{1/2}$~3.6 mins. at 5 °C and 35 s at 20 °C; Figure S23 and S24), which is typical for merocyanines in low-polarity solvents.[69] Control experiments indicated that irradiation of the *o*-fluorinated azobenzene **S1** at this wavelength (300 nm) does not result in any appreciable degree of isomerization (Figure S19 and S20). Hence, the wavelength-selectivity in this dyad stems not only from band separation (Figure S26) but also due to significant differences in the efficiency of the photoisomerization at the selected wavelengths. Merocyanine could be closed back upon irradiation at 617 nm (Figure 3d) which led to the recovery of the initial spectrum. Throughout both processes, isosbestic points were maintained at 355 nm (Figure 3c and 3d insets) proving that spiropyran **S2** can undergo unimolecular isomerization in an orthogonal manner to the azobenzene **S1**. By irradiating the mixture at 365 nm, both switches **S1** and **S2** could be isomerized at the same time with higher content of merocyanine at PSS achieved for **S1** as observed from the UV/Vis spectra (Figure 3e). The simultaneous isomerization of both **S1** and **S2** upon irradiation at 365 nm was further verified following the isomerization of individual molecules (Figure S17 and S20). Subsequent irradiation at 420 nm light led to back isomerization of both photoswitches, i.e., $Z \rightarrow E$ and open/closure isomerizations (Figure 3f) and further supported by studies on single-component mixture (Figure S18 and S22). Noteworthy throughout both processes no isosbestic points were maintained, which is consistent with the anticipated parallel photoisomerizations occurring upon irradiation of the mixture. Therefore, for this intermolecular combination of photoswitches in solution, all four states can be achieved independently (Figure 1a) which showcases the high selectivity of the photoswitching in this dyad.

The photochemical isomerization behaviour of switches **S1** and **S2** embedded in the solid **PSF** was studied with diffuse-reflectance UV/Vis (DR UV/Vis) spectroscopy (Figure 4a). In the pristine state (**State I**) **PSF** shows intense absorption above 360 nm and two bands, one at ca. 460 nm characteristic of *E*-azobenzene and a second centred at ca. 650 nm likely associated with the synthetic procedure. Brief exposure of the material to 530 nm light for 30 s led to a blue-shift of the DR UV/Vis spectrum consistent with the selective $E \rightarrow Z$ isomerization of **S1** in the solid state (Figure 4b, brown solid line, **State II**) which was accompanied by a colour change of the material (Figure 5a). Irradiation of the material at 420 nm led to the back $Z \rightarrow E$ photoisomerization of the azobenzene photoswitch accompanied by a slight amount of ring opening product of spiropyran switch **S2** (Figure 4b, orange solid line). The slight interference of spiropyran isomerization at this wave-

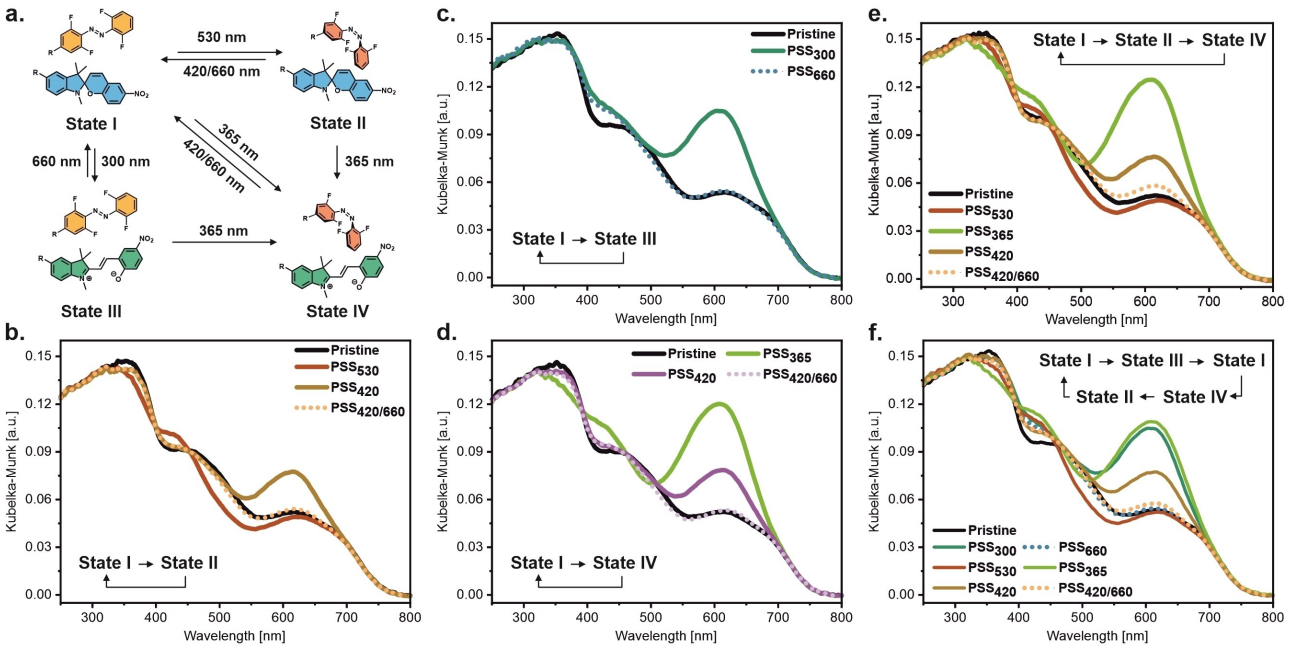

Figure 4. Orthogonal photoswitching in **PSF**. **a**. Orthogonal photoswitching upon photoexcitation of light at selective wavelengths. **b**. Reversible control of the azobenzene switch without affecting the spiropyran switch. **c**. Reversible control of the spiropyran switch without affecting the azobenzene switch. **d**. Activation and back isomerization of two photoswitches in the PSF. **e**. and **f**. Sequential control of different states in **PSF** by different wavelengths of light irradiation.

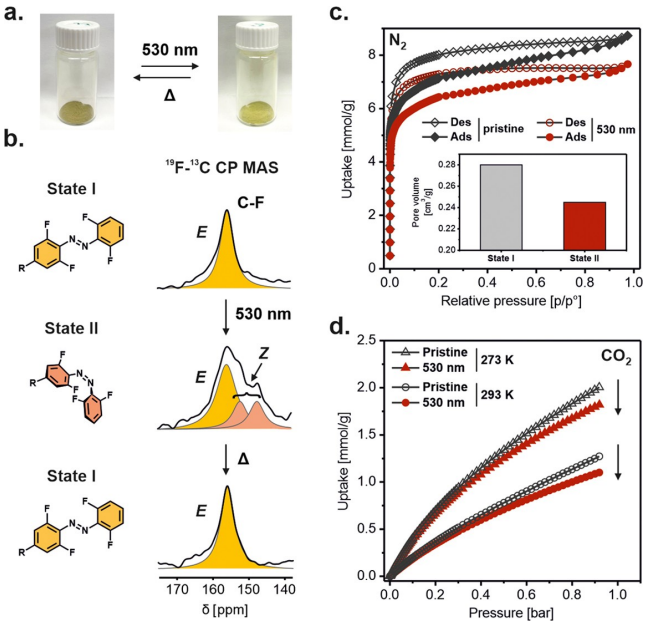

Figure 5. **a**. Color change of **PSF** in **States I** and **II**. **b**. ^{19}F–^{13}C CP MAS NMR spectra of **PSF** in **State I**, upon switching at 530 nm (**State II**) and upon reversible transformation to the pristine state **I**. **c**. N_2 adsorption isotherms at 77 K of **PSF** in **States I** (grey triangles) and **II** (red circles). **d**. CO_2 adsorption isotherms at 273 K and 293 K of **PSF** in the **States I** and **II**.

length in the material may originate either from the energy transfer between both photoswitches, or a red shift of the spiropyran absorption spectra in the solid material. Gratifying, upon subsequent irradiation of the material at 660 nm, the band characteristic of merocyanine photoswitch disappeared, indicating the cyclization of the merocyanine and thus yielding pristine material (**State I**) (Figure 4b, orange dotted line). Irradiation of the reference **PSF-S1** framework (appended exclusively with azobenzene **S1**) at 530/420 nm resulted in similar spectral changes further supporting the isomerization of the azobenzene (Figure S13a). In addition, this reversible isomerization upon alternating 530/420 nm irradiation could be performed for five cycles without any appreciable fatigue (Figure S13b), indicating the robustness of the material. Moreover, ^{13}C MAS NMR with cross-polarization (CP) from either ^{19}F or ^{1}H further corroborated the $E \rightarrow Z$ isomerization of the azobenzene in the bulk of the **PSF** material (Figure 5b, S27). The ^{19}F–^{13}C CP MAS NMR spectrum showed the resonances of fluorine-bound carbons in the 145–165 ppm region and the appearance of two new signals at $\delta = 152.3$ and 147.2 ppm characteristic of the Z isomer after irradiation at $\lambda = 530$ nm (**State II**), accounting for 38 % transformation. The isomerization was further demonstrated with ^{19}F MAS NMR, which revealed a downfield shifted resonance at −121.9 ppm (Figure S28), in agreement with ^{19}F NMR in solution (Figure S11).

Accordingly, upon irradiation of the **PSF** at 300 nm, a band characteristic of merocyanine centred at 620 nm (Figure 4c, cyan-blue solid line) was observed (**State III**), while no other spectral changes indicating the azobenzene $E \rightarrow Z$ isomerization were observed. DR UV/Vis spectroscopy revealed that the thermal isomerization of the merocyanine in the **PSF** framework follows more complex kinetics than in solution and a slight increase in the thermal stability of the

opened isomer (Figure S33). Subsequent irradiation at 660 nm led to a recovery of the pristine spectra (**State I**, Figure 4c, blue dotted line), demonstrating selective and reversible isomerization of spiropyran switch **S2** in the **PSF** framework. Similar spectral changes were observed in the reference **PSF-S2** material upon irradiation at either 300 or 365 nm light (Figure S14b,c), with limited fatigue observed upon cycling (Figure S14d). **State IV** was achieved upon irradiation of the **PSF** material at 365 nm, which led to the isomerization of both photoswitches appended to the framework. Indeed, the decrease in the band centered at 350 nm and blue-shift of the band centered at 475 nm consistent with $E \rightarrow Z$ isomerization of azobenzene along with the emergence of the band cantered at 600 nm characteristic of the ring-opened merocyanine was observed (Figure 4d, light-green solid line), demonstrating isomerization of both switches in the solid. Subsequent irradiation at 420 nm induced near quantitative $Z \rightarrow E$ back photoisomerization of azobenzene as well as partial recovery of the spiropyran photoswitch (Figure 4d, violet solid line). This observation is consistent with the result obtained during **State II**→**State I** isomerization upon irradiation at 420 nm, which resulted in the formation of a small amount of the ring-opened merocyanine (Figure 4b, orange solid line). All these spectral changes are consistent with those observed in solution and support high wavelength-selectivity of the **S1**/**S2** photoswitch dyad in the solid state. However, contrary to the solution, in the photostationary state achieved upon irradiation of the material at 420 nm, a small amount of the merocyanine form is present along with the *E*-azobenzene pendants. Nevertheless, the pristine state (**State I**) can be recovered upon irradiation of the material at 660 nm (Figure 4d, pink dotted line). All these transformations were further supported by the characteristic changes in DRIFT spectra occurring upon isomerization (Figure S15 and S16). These results unambiguously confirmed the achievement of high selectivity in the control of two distinct photoswitches in the solid porous framework. To further showcase, the complexity and diversity of this system through distinct wavelength modulation, a series of sequential irradiations at distinct wavelengths was performed. A sequential irradiation at $\lambda = 530$ nm→365 nm →420 nm/660 nm triggers a sequential isomerization between distinct states of the material in order **State I**→**State II**→**State IV**→**State I** (Figure 4e). In another sequence $\lambda = 300$ nm→660 nm→530 nm→365 nm→420 nm→420 nm/660 nm, the state of the material can be interconverted following **State I**→**State III**→**State I**→**State IV**→**State II**→**State I** (Figure 4f). Hence, the incorporation of multiple wavelength-orthogonal photoswitches in porous frameworks, as demonstrated here, can be of great value for future smart materials to achieve selective and non-invasive control over multi-state materials' properties by light manipulation.

The selective photoswitching of the pendants at the molecular level was accompanied by a drastic change of the material porosity from **State I** to **II** (pore volume reduction of 12.5 %), as demonstrated by N_2 adsorption isotherms at 77 K (Figure 5c, S30 and Table S4). Prompted by this efficiency of porosity modulation, CO_2 adsorption isotherms under mild conditions (273 K and 293 K) and pressure (up to 1 bar) (Figure 5d, S31 and S32) were collected. Notably, the amount of CO_2 adsorbed by the **PSF** was reduced by 9 mol % at 273 K and reached 14 % at 293 K upon irradiation at 530 nm (**State II**), enabling the modulation of macroscopic properties by a molecular switching.

In conclusion, this study represents the first demonstration of an orthogonal photoswitching system incorporated in the solid state. We successfully integrated two photoswitches, i.e. *o*-fluoroazobenzene and nitro-spiropyran, into a porous aromatic framework. Notably, both candidates exhibited excellent photoisomerization performance, both in an intermolecular system and integrated into a solid porous material. Through light manipulation, we achieved orthogonal control over their isomerization, enabling us to reversibly alter the material's four distinct states and sequential interconversion between multiple distinct states. The photoisomerization was further quantified in the bulk material by selective solid-state NMR detection of the azobenzene switches. The isomerization of appended photoswitches impacted the macroscopic properties, modulating the adsorption capacity of N_2 and CO_2. This work serves as a crucial proof-of-concept, guiding the design of the future responsive materials. This achievement represents a significant advancement in the field of light-responsive materials and paves the way for the development of more sophisticated and versatile smart materials with multiple controllable states. Furthermore, the combination of these two photoswitches can be extended to other scaffolds, including liquid crystal networks, gels, and block copolymers. Future efforts should be focused on increasing the concentration of switchable units in the material, engineering cooperativity effects between the switches and the material backbone and extending this concept to other wavelength-orthogonal photoactive units.

Author Contributions

J.S., W.D. and B.L.F. conceived the project. B.L.F., A.C. and W. D. guided and supervised the research. W.D., J.S. and P.C. designed the pair of photoswitches. J.S. and P.C. synthesized the building blocks and all materials. J.S. carried out the UV and NMR irradiation studies in solution. J.S. carried out the SEM measurements. J.S. performed DR-UV/Vis and FT-IR measurements. J.P. performed thermogravimetric analysis, gas adsorption isotherms. S.B. carried out solid-state NMR spectra. J.S. and W.D. wrote the initial manuscript. P.C. designed and made all the graphics. All authors discussed the results and commented on the manuscript.

Acknowledgements

This work was supported from the following sources: China Scholarship Council (CSC PhD Fellowship No. 201808330459 to J.S.), the Ministry of Education, Culture and Science of the Netherlands (Gravitation Program No.

024.001.035 to BLF), Financial support from The Netherlands Organization for Scientific Research (NWO-CW), the European Research Council (ERC; advanced Grant No. 694345 to B.L.F.). PRIN (SHERPA 2020 No. H45F21003430001) and PRIN (HySTAR 2022 No. H53D23004720006) and Lombardy Region for "Enhancing Photosynthesis" grant (2021-2023 No. H45F21002830007). W.D. is grateful for financial support from Marie Skłodowska-Curie Actions (Individual Fellowship No. 101027639). P.C. is grateful for the financial support provided by the PRELUDIUM grant from the National Science Center Poland (Reg. No: 2023/49/N/ST5/01864).

Conflict of Interest

The authors declare no competing financial interests.

Data Availability Statement

The data that support the findings of this study are available in the supplementary material of this article.

Keywords: Molecular switch · Solid-state isomerization · Spiropyran · Azobenzene · Orthogonal photoswitching

[1] W. R. Browne, B. L. Feringa, *Molecular Switches*, Wiley-VCH, Weinheim, Germany **2011**.
[2] Z. L. Pianowski, Ed., *Molecular Photoswitches: Chemistry, Properties, and Applications*, Wiley-VCH, Weinheim **2022**.
[3] A. Fihey, A. Perrier, W. R. Browne, D. Jacquemin, *Chem. Soc. Rev.* **2015**, *44*, 3719–3759.
[4] M. Jeong, J. Park, S. Kwon, *Eur. J. Org. Chem.* **2020**, *2020*, 7254–7283.
[5] E. H. Discekici, J. Read de Alaniz, *ACS Cent. Sci.* **2018**, *4*, 1087–1088.
[6] J. Sheng, D. R. S. Pooler, B. L. Feringa, *Chem. Soc. Rev.* **2023**, *52*, 5875–5891.
[7] F. Tian, D. Jiao, F. Biedermann, O. A. Scherman, *Nat. Commun.* **2012**, *3*, 1207.
[8] M. A. C. Stuart, W. T. S. Huck, J. Genzer, M. Müller, C. Ober, M. Stamm, G. B. Sukhorukov, I. Szleifer, V. V. Tsukruk, M. Urban, F. Winnik, S. Zauscher, I. Luzinov, S. Minko, *Nat. Mater.* **2010**, *9*, 101–113.
[9] J. Zhuang, M. R. Gordon, J. Ventura, L. Li, S. Thayumanavan, *Chem. Soc. Rev.* **2013**, *42*, 7421.
[10] P. Theato, B. S. Sumerlin, R. K. O'Reilly, T. H. Epp, *Chem. Soc. Rev.* **2013**, *42*, 7055–7056.
[11] M. Wei, Y. Gao, X. Li, M. J. Serpe, *Polym. Chem.* **2017**, *8*, 127–143.
[12] X. Fu, L. Hosta-Rigau, R. Chandrawati, J. Cui, *Chem* **2018**, *4*, 2084–2107.
[13] A. Blanc, C. G. Bochet, *J. Org. Chem.* **2002**, *67*, 5567–5577.
[14] P. W. Kamm, L. L. Rodrigues, S. L. Walden, J. P. Blinco, A.-N. Unterreiner, C. Barner-Kowollik, *Chem. Sci.* **2022**, *13*, 531–535.
[15] K. Hiltebrandt, T. Pauloehrl, J. P. Blinco, K. Linkert, H. G. Börner, C. Barner-Kowollik, *Angew. Chem. Int. Ed.* **2015**, *54*, 2838–2843.
[16] V. X. Truong, J. Bachmann, A. Unterreiner, J. P. Blinco, C. Barner-Kowollik, *Angew. Chem. Int. Ed.* **2022**, *61*, e202113076.
[17] L. García-Fernández, C. Herbivo, V. S. M. Arranz, D. Warther, L. Donato, A. Specht, A. Del Campo, *Adv. Mater.* **2014**, *26*, 5012–5017.
[18] Y. Fu, N. A. Simeth, R. Toyoda, R. Brilmayer, W. Szymanski, B. L. Feringa, *Angew. Chem.* **2023**, *135*, e202218203.
[19] F. M. Raymo, M. Tomasulo, *Chem. Soc. Rev.* **2005**, *34*, 327.
[20] J. Andréasson, S. D. Straight, T. A. Moore, A. L. Moore, D. Gust, *J. Am. Chem. Soc.* **2008**, *130*, 11122–11128.
[21] J. Andréasson, U. Pischel, S. D. Straight, T. A. Moore, A. L. Moore, D. Gust, *J. Am. Chem. Soc.* **2011**, *133*, 11641–11648.
[22] M. Bälter, S. Li, J. R. Nilsson, J. Andréasson, U. Pischel, *J. Am. Chem. Soc.* **2013**, *135*, 10230–10233.
[23] N. M.-W. Wu, M. Ng, V. W.-W. Yam, *Nat. Commun.* **2022**, *13*, 33.
[24] M. M. Lerch, M. J. Hansen, W. A. Velema, W. Szymanski, B. L. Feringa, *Nat. Commun.* **2016**, *7*, 12054.
[25] F. Zhao, L. Grubert, S. Hecht, D. Bléger, *Chem. Commun.* **2017**, *53*, 3323–3326.
[26] M. Li, S. Yang, W. Liang, X. Zhang, D. Qu, *Dyes Pigm.* **2019**, *166*, 239–244.
[27] H. Nishioka, X. Liang, T. Kato, H. Asanuma, *Angew. Chem. Int. Ed.* **2012**, *51*, 1165–1168.
[28] D. Manna, T. Udayabhaskararao, H. Zhao, R. Klajn, *Angew. Chem. Int. Ed.* **2015**, *54*, 12394–12397.
[29] H. Dube, J. Rebek, *Angew. Chem. Int. Ed.* **2012**, *51*, 3207–3210.
[30] Z. Hong-Cai, L. Jeffrey R, Y. Omar M, *Chem. Rev.* **2012**, *112*, 673–674.
[31] X. Feng, X. Ding, D. Jiang, *Chem. Soc. Rev.* **2012**, *41*, 6010–6022.
[32] Y. Tian, G. Zhu, *Chem. Rev.* **2020**, *120*, 8934–8986.
[33] H. Furukawa, K. E. Cordova, M. O'Keeffe, O. M. Yaghi, *Science* **2013**, *341*, DOI 10.1126/science.1230444.
[34] S. Das, P. Heasman, T. Ben, S. Qiu, *Chem. Rev.* **2017**, *117*, 1515–1563.
[35] Y. Yuan, G. Zhu, *ACS Cent. Sci.* **2019**, *5*, 409–418.
[36] W. Danowski, T. Van Leeuwen, W. R. Browne, B. L. Feringa, *Nanoscale Adv.* **2021**, *3*, 24–40.
[37] V. Ramamurthy, *Acc. Chem. Res.* **2015**, *48*, 2904–2917.
[38] M. Grzelczak, L. M. Liz-Marzán, R. Klajn, *Chem. Soc. Rev.* **2019**, *48*, 1342–1361.
[39] O. B. Berryman, H. Dube, J. Rebek, *Isr. J. Chem.* **2011**, *51*, 700–709.
[40] A. B. Grommet, L. M. Lee, R. Klajn, *Acc. Chem. Res.* **2020**, *53*, 2600–2610.
[41] J. Gemen, J. R. Church, T.-P. Ruoko, N. Durandin, M. J. Białek, M. Weißenfels, M. Feller, M. Kazes, M. Odaybat, V. A. Borin, R. Kalepu, Y. Diskin-Posner, D. Oron, M. J. Fuchter, A. Priimagi, I. Schapiro, R. Klajn, *Science* **2023**, *381*, 1357–1363.
[42] J. Hou, A. Mondal, G. Long, L. Haan, W. Zhao, G. Zhou, D. Liu, D. J. Broer, J. Chen, B. L. Feringa, *Angew. Chem. Int. Ed.* **2021**, *60*, 8251–8257.
[43] J. Hou, G. Long, W. Zhao, G. Zhou, D. Liu, D. J. Broer, B. L. Feringa, J. Chen, *J. Am. Chem. Soc.* **2022**, *144*, 6851–6860.
[44] F. Castiglioni, W. Danowski, J. Perego, F. K. C. Leung, P. Sozzani, S. Bracco, S. J. Wezenberg, A. Comotti, B. L. Feringa, *Nat. Chem.* **2020**, *12*, 595–602.
[45] M. R. A. Bhatti, A. Kernin, M. Tausif, H. Zhang, D. Papageorgiou, E. Bilotti, T. Peijs, C. W. M. Bastiaansen, *Adv. Opt. Mater.* **2022**, *10*, 2102186.
[46] S. Krause, B. L. Feringa, *Nat. Chem. Rev.* **2020**, *4*, 550–562.
[47] P. K. Kundu, G. L. Olsen, V. Kiss, R. Klajn, *Nat. Commun.* **2014**, *5*, 3588.
[48] D. E. Williams, C. R. Martin, E. A. Dolgopolova, A. Swifton, D. C. Godfrey, O. A. Ejegbavwo, P. J. Pellechia, M. D. Smith, N. B. Shustova, *J. Am. Chem. Soc.* **2018**, *140*, 7611–7622.

[49] S. Garg, H. Schwartz, M. Kozlowska, A. B. Kanj, K. Müller, W. Wenzel, U. Ruschewitz, L. Heinke, *Angew. Chem. Int. Ed.* **2019**, *58*, 1193–1197.
[50] C. R. Martin, K. C. Park, G. A. Leith, J. Yu, A. Mathur, G. R. Wilson, G. B. Gange, E. L. Barth, R. T. Ly, O. M. Manley, K. L. Forrester, S. G. Karakalos, M. D. Smith, T. M. Makris, A. K. Vannucci, D. V. Peryshkov, N. B. Shustova, *J. Am. Chem. Soc.* **2022**, *144*, 4457–4468.
[51] G. Das, T. Prakasam, N. Alkhatib, R. G. AbdulHalim, F. Chandra, S. K. Sharma, B. Garai, S. Varghese, M. A. Addicoat, F. Ravaux, R. Pasricha, R. Jagannathan, N. Saleh, S. Kirmizialtin, M. A. Olson, A. Trabolsi, *Nat. Commun.* **2023**, *14*, 3765.
[52] G. C. Thaggard, G. A. Leith, D. Sosnin, C. R. Martin, K. C. Park, M. K. McBride, J. Lim, B. J. Yarbrough, B. K. P. Maldeni Kankanamalage, G. R. Wilson, A. R. Hill, M. D. Smith, S. Garashchuk, A. B. Greytak, I. Aprahamian, N. B. Shustova, *Angew. Chem. Int. Ed.* **2023**, *62*, e202211776.
[53] J. Sheng, J. Perego, S. Bracco, W. Czepa, W. Danowski, S. Krause, P. Sozzani, A. Ciesielski, A. Comotti, B. L. Feringa, *Adv. Mater.* **2024**, *36*, 2305783.
[54] S. Krause, J. D. Evans, V. Bon, S. Crespi, W. Danowski, W. R. Browne, S. Ehrling, F. Walenszus, D. Wallacher, N. Grimm, D. M. Többens, M. S. Weiss, S. Kaskel, B. L. Feringa, *Nat. Commun.* **2022**, *13*, 1951.
[55] M. Baroncini, S. D'Agostino, G. Bergamini, P. Ceroni, A. Comotti, P. Sozzani, I. Bassanetti, F. Grepioni, T. M. Hernandez, S. Silvi, M. Venturi, A. Credi, *Nat. Chem.* **2015**, *7*, 634–640.
[56] G. Das, T. Prakasam, M. A. Addicoat, S. K. Sharma, F. Ravaux, R. Mathew, M. Baias, R. Jagannathan, M. A. Olson, A. Trabolsi, *J. Am. Chem. Soc.* **2019**, *141*, 19078–19087.
[57] J. Park, D. Yuan, K. T. Pham, J. R. Li, A. Yakovenko, H. C. Zhou, *J. Am. Chem. Soc.* **2012**, *134*, 99–102.
[58] C. Bin Fan, L. Le Gong, L. Huang, F. Luo, R. Krishna, X. F. Yi, A. M. Zheng, L. Zhang, S. Z. Pu, X. F. Feng, M. B. Luo, G. C. Guo, *Angew. Chem. Int. Ed.* **2017**, *56*, 7900–7906.
[59] Y. Zheng, H. Sato, P. Wu, H. J. Jeon, R. Matsuda, S. Kitagawa, *Nat. Commun.* **2017**, *8*, 100.
[60] F. Luo, C. Bin Fan, M. B. Luo, X. L. Wu, Y. Zhu, S. Z. Pu, W. Y. Xu, G. C. Guo, *Angew. Chem. Int. Ed.* **2014**, *53*, 9298–9301.
[61] W. Danowski, T. van Leeuwen, S. Abdolahzadeh, D. Roke, W. R. Browne, S. J. Wezenberg, B. L. Feringa, *Nat. Nanotechnol.* **2019**, *14*, 488–494.
[62] W. Danowski, F. Castiglioni, A. S. Sardjan, S. Krause, L. Pfeifer, D. Roke, A. Comotti, W. R. Browne, B. L. Feringa, *J. Am. Chem. Soc.* **2020**, *142*, 9048–9056.
[63] J. Sheng, W. Danowski, S. Crespi, A. Guinart, X. Chen, C. Stähler, B. L. Feringa, *Chem. Sci.* **2023**, *14*, 4328–4336.
[64] C. Stähler, L. Grunenberg, M. W. Terban, W. R. Browne, D. Doellerer, M. Kathan, M. Etter, B. V. Lotsch, B. L. Feringa, S. Krause, *Chem. Sci.* **2022**, *13*, 8253–8264.
[65] J. Sheng, J. Perego, W. Danowski, S. Bracco, S. Chen, X. Zhu, C. X. Bezuidenhout, S. Krause, W. R. Browne, P. Sozzani, A. Comotti, B. L. Feringa, *Chem* **2023**, *9*, 2701–2716.
[66] G. R. Wilson, K. C. Park, G. C. Thaggard, C. R. Martin, A. R. Hill, J. Haimerl, J. Lim, B. K. P. Maldeni Kankanamalage, B. J. Yarbrough, K. L. Forrester, R. A. Fischer, P. J. Pellechia, M. D. Smith, S. Garashchuk, N. B. Shustova, *Angew. Chem. Int. Ed.* **2023**, *62*, e202308715.
[67] D. Bléger, J. Schwarz, A. M. Brouwer, S. Hecht, *J. Am. Chem. Soc.* **2012**, *134*, 20597–20600.
[68] L. Kortekaas, W. R. Browne, *Chem. Soc. Rev.* **2019**, *48*, 3406–3424.
[69] N. Turetta, W. Danowski, L. Cusin, P. A. Livio, R. Hallani, I. McCulloch, P. Samorì, *J. Mater. Chem. C* **2023**, *11*, 7982–7988.

Manuscript received: March 11, 2024
Accepted manuscript online: March 26, 2024
Version of record online: ■■, ■■

Research Articles

Molecular Switches

J. Sheng, J. Perego, S. Bracco, P. Cieciórski, W. Danowski,* A. Comotti,* B. L. Feringa* **e202404878**

Orthogonal Photoswitching in a Porous Organic Framework

Orthogonal photoswitching

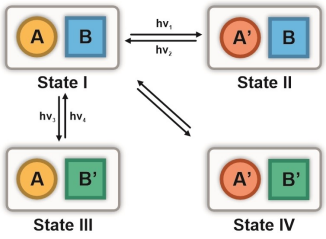

Two photoswitches, i.e., 6-nitro-spiropyran and *o*-fluoroazobenzene are shown to operate in a wavelength-orthogonal manner both in solution and when integrated into a porous material scaffold. Selective isomerization of each photoswitch can be triggered by a specific wavelength of light giving rise to four independently accessible states of the porous material, thus providing a basis for the dynamic multifunctional materials.